Chemistry
A European
Journal

Chemistry Europe
European Chemical Societies Publishing

Accepted Article

Title: γ-Resorcyclic Acid-Based AIEgens for Illuminating Endoplasmic Reticulum

Authors: Jaypalsing Ingle, Hiren Dedaniya, Chaithra Mayya, Anirban Mondal, Dhiraj Bhatia, and Sudipta Basu

To be cited as: *Chem. Eur. J.* **2022**, e202200203

Link to VoR: https://doi.org/10.1002/chem.202200203

WILEY-VCH

10.1002/chem.202200203

WILEY-VCH

RESEARCH ARTICLE

γ-Resorcyclic Acid-Based AIEgens for Illuminating Endoplasmic Reticulum**

Jaypalsing Ingle,[a] Hiren Dedaniya,[a]‡ Chaithra Mayya,[b]‡ Anirban Mondal,[a] Dhiraj Bhatia,[b] Sudipta Basu*[a]

[a] J. Ingle, H. Dedaniya, Prof. A. Mondal, Prof. S. Basu
Discipline of Chemistry, Indian Institute of Technology Gandhinagar, Palaj, Gujarat, 382355, India
E-mail: Sudipta.basu@iitgn.ac.in; Twitter: @iitgn
[b] C. Mayya, Prof. D. Bhatia
Discipline of Biological Engineering, Indian Institute of Technology Gandhinagar, Palaj, Gujarat, 382355, India
‡ These authors contributed equally

Supporting information for this article is given via a link at the end of the document.

** **AIE=aggregation-induced emission**

Abstract: Endoplasmic reticulum (ER) has emerged as one of the interesting sub-cellular organelles due to its role in myriads of biological phenomena. Subsequently, visualization of the structure-function and dynamics of ER remained a major challenge to understand its involvement in different diseased states including cancer. To illuminate the ER, herein we have designed and synthesized γ-resorcyclic acid-based small molecules which showed remarkable aggregation induced emission (AIE) property in water. This AIE property was originated from the dual intramolecular H-bonding leading to the self-assembled 2D aggregation confirmed by the pH and temperature dependent fluorescence quenching studies as well as scanning electron microscopy. These small molecules illuminated the sub-cellular ER in HeLa cervical cancer cells as well as non-cancerous RPE-1 human retinal epithelial cells within 1h. These novel small molecules have the potential to light up ER chemical biology in diseased states.

Introduction

Endoplasmic reticulum (ER), the largest membrane bound sub-cellular organelle acts as the protein and lipid synthesis hub.[1-4] ER also regulates protein processing through post-translational modifications, which if disrupted, leads to the stress accumulation (ER stress) inside the cells.[5-7] This ER stress is highly instrumental in several disease states including cancer.[8-12] As a result, visualization of the structure, functions and dynamics of ER is of utmost importance to understand its role in cancer development and progression.[13,14]

Consequently, fluorescent dyes are developed with variable organelle selectivity, tedious synthetic steps and cumbersome purification protocols.[15-17] Moreover, these fluorescent probes suffer photobleaching, aggregation caused quenching (ACQ) and moderate to high toxicity at staining concentration.[18-20] To overcome these challenges, aggregation-induced emission probes (AIEgens) have emerged as novel tools for biomedical imaging.[21-24] Till date, tetraphenylethylene (TPE) and hexaphenylsilol (HPS)-based AIEgens have been used extensively for bioimaging, despite their hydrophobic nature, cumbersome synthesis and purification.[25-27] In spite of having tremendous potential to light-up cell membrane and sub-cellular organelles,[28-32] development of novel biocompatible small

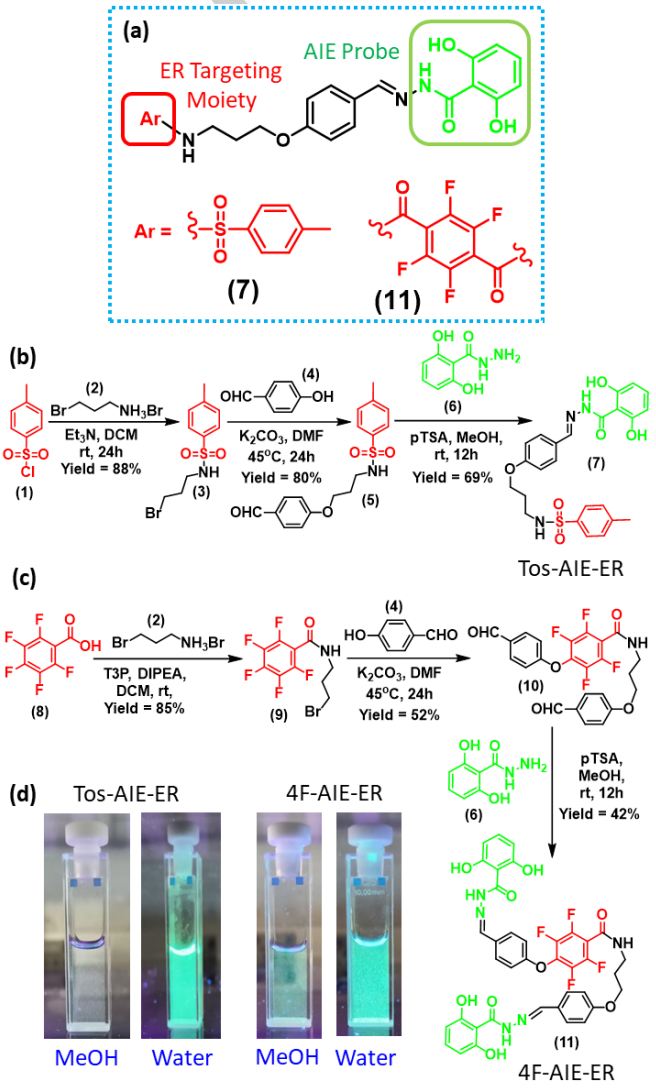

Figure 1. (a) Design of ER targeting AIE molecules. (b, c) Synthetic schemes of γ-resorcyclic acid based AIEgens (d) Images of AIE property of Tos-AIE-ER and 4F-AIE-ER in methanol and water under UV light.

10.1002/chem.202200203

molecule AIEgens for selective illumination of ER remained elusive and limited.[33-35]

To address this, herein, we rationally designed and synthesized γ-resorcyclic acid-based small molecules through easy and concise strategy having p-toluene sulfonic acid and pentafluorobenzoic acid moieties for ER localization (Figure 1a). These small molecules demonstrated remarkable aggregation-induced emission (AIE) properties in water through dual-intramolecular H-bonding to restrict intramolecular motion (RIM) in aggregated state. The AIE property was confirmed by disruption of dual H-bonding in pH and temperature dependent studies leading to quenching of the fluorescence emission. These small molecules illuminated the sub-cellular ER in HeLa cervical cancer cells as well as non-cancerous human retinal epithelial cells (RPE-1) observed by fluorescence microscopy. These novel small molecules have the potential to light up ER chemical biology in different diseases states.

Results and Discussion

For the successful development of ER targeting AIEgens, the molecules must possess an AIE active moiety tagged with ER localizing moiety. To address this, we have chosen γ-resorcyclic acid as the AIE active moiety [36] linked with p-Toluenesulfonamide [37-39] and pentafluorobenzoic acid [40, 41] as ER localizing moiety (Figure 1a). The synthetic scheme of γ-resorcyclic acid-based ER targeting AIEgens (7 and 11) is outlined in Figure 1b and 1c. In short, p-toluene sulfonylchloride (1) was reacted with 3-bromo-propylamine (2) in presence of triethylamine as base to attain 3-bromo-propyl-tosylamine (3) in 88% yield, which was further reacted with 4-hydroxy-benzaldehyde (4) in presence of K_2CO_3 as base to obtain compound 5 in 80% yield. The tosyl-benzaldehyde derivative 5 was reacted with γ-resorcyclic acid-hydrazide (6) in presence of p-toluene sulfonic acid (pTSA) as catalyst to afford γ-resorcyclic acid-hydrazide-hydrazone-p-Tosyl derivative (7) (Tos-AIE-ER) in 69% yield.[36] Similarly, pentafluorobenzoic acid (8) was conjugated with 3-bromo-propylamine (2) in presence of propylphosphonic anhydride (T3P) as coupling agent to obtain pentafluorobenzoic acid-bromo-propylamine conjugate (9) in 85% yield followed by reaction with 4-hydroxy-benzaldehyde (4) in presence of K_2CO_3. Unexpectedly, we obtained the tetrafluoro-benzoic acid derivative 10 through replacement of both bromo and 4-fluoro groups by 4-hydroxy-benzadelhyde in 52% yield. Finally, we reacted compound 10 with γ-resorcyclic acid-hydrazide (6) in presence of pTSA as catalyst to acquire γ-resorcyclic acid-hydrazide-hydrazone-tetrafluoro-benzoic acid derivative (11) (4F-AIE-ER) in 42% yield. The structures of all the intermediates and the final products were confirmed by ^{1}H, ^{13}C, ^{19}F NMR and HR-MS spectroscopy (Figure S1-S18). In our previous study, we observed that γ-resorcyclic acid-hydrazide-hydrazone-based small molecules demonstrated notable AIE property in solid state as well as in water due to the presence of dual intramolecular H-bonding.[36] Hence, we evaluated the emission property of Tos-AIE-ER and 4F-AIE-ER in methanol which showed negligible emission. However, both the compounds showed remarkable fluorescence emission in water as well as in solid state under long range UV light (Figure 1d, Figure S19), which clearly indicated the AIE property.

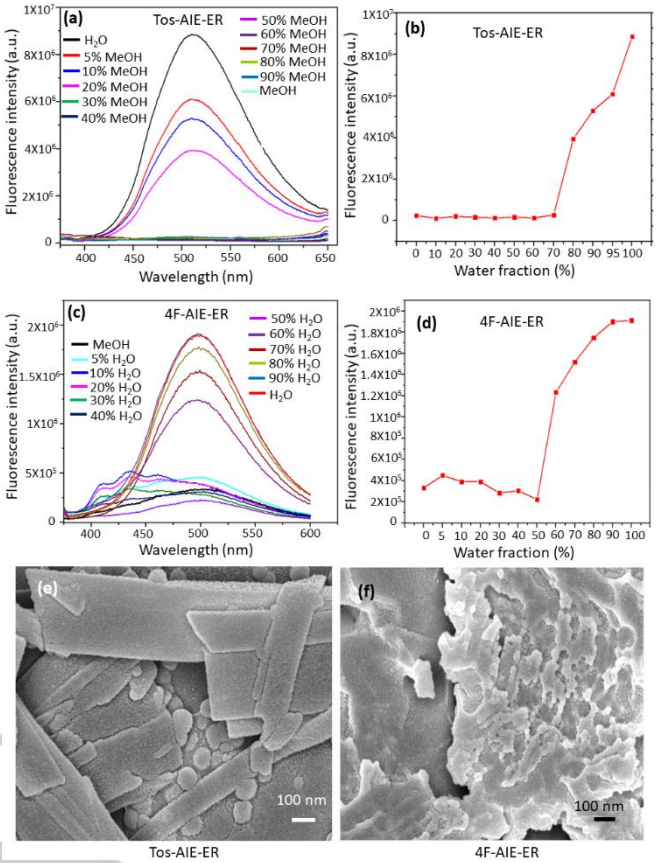

Figure 2. (a, c) Fluorescence emission spectra of Tos-AIE-ER and 4F-AIE-ER in different methanol: water. (b, d) Florescence emission intensity (λ_{max} = 512 and 502 nm) versus water fraction graph of Tos-AIE-ER and 4F-AIE-ER respectively in different methanol: water mixture. (e, f) FESEM images of Tos-AIE-ER and 4F-AIE-ER in water respectively.

To understand the binary solvent ratio for AIE, we dissolved both the compounds (Tos-AIE-ER and 4F-AIE-ER) in methanol and titrated with water. Tos-AIE-ER showed no measurable fluorescence emission until methanol: water = 30:70 (v/v) (Figure 2a, b and Figure S20). However, Tos-AIE-ER demonstrated increase in fluorescence emission at λ_{max} = 512 nm for methanol: water = 20:80 with significant increase in 100% water. Similarly, 4F-AIE-ER showed weak fluorescence emission till methanol: water = 50:50 (v/v), with increase in 40:60 methanol: water (v/v) at λ_{max} = 502 nm (Figure 2c, d, Figure S21). 4F-AIE-ER also showed significant increase in fluorescence emission in 100% water. The UV-Vis spectra of Tos-AIE-ER displayed absorption at λ_{max} = 337 nm and 330 nm in methanol and water, whereas 4F-AIE-ER displayed absorption at λ_{max} = 320 nm and 313 nm in methanol and water respectively (Figure S22). We also calculated the molar absorption coefficients (ε) from Beer-Lambert Law for Tos-AIE-ER and 4F-AIE-ER which were found to be ε = 4365 M^{-1} cm^{-1} and 11570 $M^{-1}cm^{-1}$ respectively at λ_{max} = 330 nm and 313 nm respectively. Both the compounds indicated large Stokes shift of 182-189 nm with marginal overlap between absorption and emission spectra, which is ideal for fluorescence imaging. We calculated the fluorescence quantum yield of the Tos-AIE-ER and 4F-AIE-ER in water which was found to be 7.64% and 3.15% respectively. Much less quantum yield (0.11% and 0.12% respectively) of Tos-AIE-ER and 4F-AIE-ER in methanol was observed. We anticipate that, both Tos-AIE-ER and 4F-AIE-ER

10.1002/chem.202200203

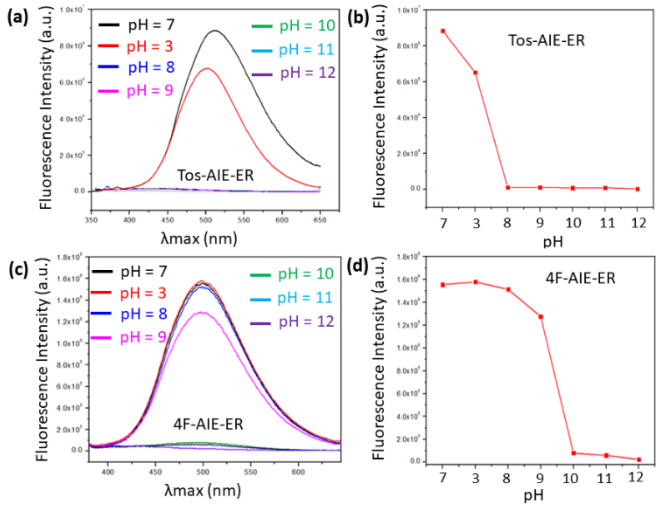

Figure 3. (a, c) Fluorescence emission spectra of Tos-AIE-ER and 4F-AIE-ER in different pH. (b, d) Florescence emission intensity (λ_{max} = 512 and 502 nm) versus pH graph of Tos-AIE-ER and 4F-AIE-ER respectively.

form strong intermolecular H-bonding with polar protic solvent methanol leading to complete solubility of both the molecules without any aggregation. As a result, both the molecules lack the dual intramolecular H-bonding for the restriction of the intramolecular motion (RIM) which is the underlying mechanism for AIE activity of Tos-AIE-ER and 4F-AIE-ER. The aggregation of Tos-AIE-ER and 4F-AIE-ER were also confirmed by field-emission scanning electron microscopy (FESEM). The FESEM images (Figure 2e, f) clearly showed that both the compounds aggregated into two-dimensional sheet like structures in water. These fluorescence spectroscopy and electron microscopy evidently confirmed the AIE property of Tos-AIE-ER and 4F-AIE-ER in water.

To confirm that dual intramolecular H-bonding as the underlying mechanism to restrict the intramolecular motion (RIM) leading to the AIE property, we disrupted the H-bonding in higher pH.[36] We evaluated the fluorescence emission at λ_{max} = 512 nm of Tos-AIE-ER in a pH dependent manner from pH = 7 to 12. We observed a remarkable decrease in fluorescence emission at basic pH (from pH = 8 to 12) (Figure 3a, b and Figure S23). Interestingly, Tos-AIE-ER regained its fluorescence emission property at acidic pH = 3. Similarly, 4F-AIE-ER also demonstrated a pH dependent decrease in fluorescence intensity at λ_{max} = 502 nm from pH = 7 to 9. However, at pH 10 to 12, 4F-AIE-ER showed a remarkable fluorescence emission reduction (Figure 3c, d and Figure S24). The fluorescence emission was recovered back to 4F-AIE-ER in pH = 3. Furthermore, the weak intramolecular H-bonding can also be disrupted by increasing the temperature causing increased intramolecular motion, leading to the reduction in AIE property.[36, 42] Hence, we assessed the fluorescence emission of Tos-AIE-ER and 4F-AIE-ER in a temperature dependent manner from 25°C to 80°C. Fascinatingly, we observed a significant gradual decline in fluorescence emission for both the compounds with increase in temperature (Figure S25, S26). Furthermore, these fluorescence quenching observations were reversible for both the compounds. To be successful in bioimaging, the AIE molecules should show fluorescence emission in physiological temperature (37 °C) for longer time. Hence, we incubated Tos-AIE-ER and 4F-AIE-ER in water at 37 °C in a time dependent manner (1h, 6h, 12h and 24h)

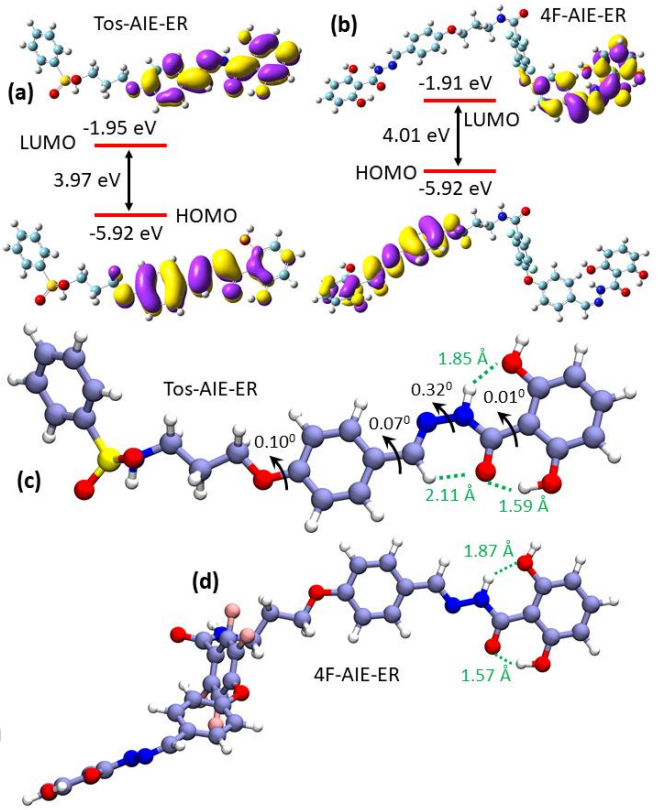

Figure 4. (a, b) Energy level diagram of frontier molecular orbitals, HOMO and, LUMO of Tos-AIE-ER and 4F-AIE-ER respectively in water, estimated from DFT calculation. The isodensity surface plots of frontier molecular orbitals are shown with an isovalue of 0.02 a.u. (c, d) Optimized geometry of Tos-AIE-ER and 4F-AIE-ER respectively obtained from B3LYP/6-31+G(d,p) level of theory. Hydrogen bonding is shown in green dotted lines whereas the dihedral angles are represented by black arrows. Color coding of atoms: C: ice blue; hydrogen: white; nitrogen: blue; oxygen: red; sulfur: yellow; fluorine: pink.

and measured the fluorescence emission at λ_{max} = 512 and 502 nm respectively. We observed no significant change in the fluorescence emission intensity over 24h at 37 °C in water for both the compounds (Figure S27). These pH and temperature dependent assays evidently confirmed that intramolecular dual H-bonding as the underlying mechanism for the AIE properties shown by Tos-AIE-ER and 4F-AIE-ER.

We used density functional theory (DFT) to measure the frontier molecular orbitals and the energy gaps between HOMO and LUMO of Tos-AIE-ER and 4F-AIE-ER in water and methanol. The calculated energy differences were found to be 3.97 eV (213.5 nm) and 4.01 eV (308.6 nm) for Tos-AIE-ER and 4F-AIE-ER respectively in water (Figure 4a, b) which were correlating with the measured UV-Vis absorbance wavelength. In methanol, the energy differences between HOMO and LUMO were found to be also 3.97 eV and 4.07 eV for Tos-AIE-ER and 4F-AIE-ER respectively (Figure S28). To further understand the AIE property, Gaussian 09 program[43] was used to perform the density functional theory (DFT) based calculations. The geometries of Tos-AIE-ER and 4f-AIE-ER were optimized by employing the B3LYP hybrid density functional in combination with the 6-31+G(d,p) basis set.[44] The presence of solvent was mimicked with the universal continuum model, SMD.[45] The optimized

10.1002/chem.202200203

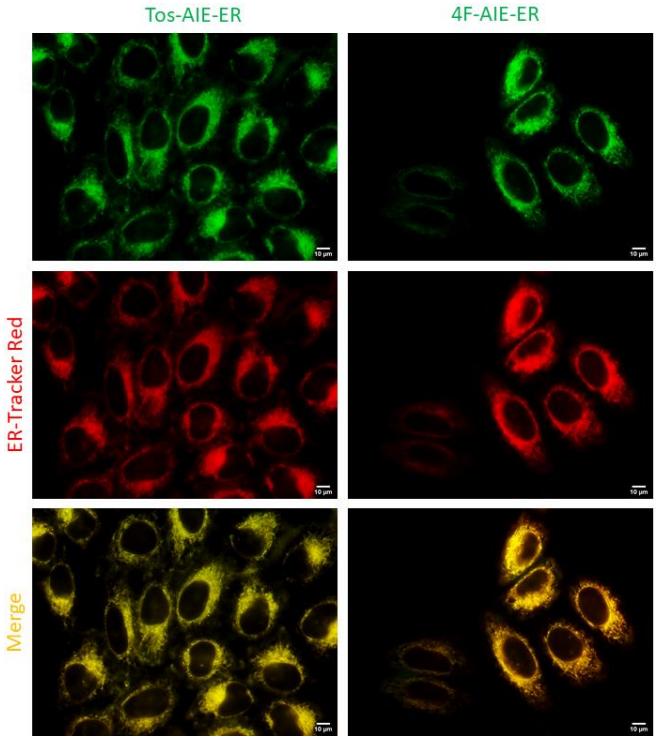

Figure 5. Fluorescence microscopy images of HeLa cells incubated with Tos-AIE-ER and 4F-AIE-ER at 20 μM concentration for 1h at 37°C, followed by staining the ER with ER Tracker Red dye. Scale bar = 10 μm.

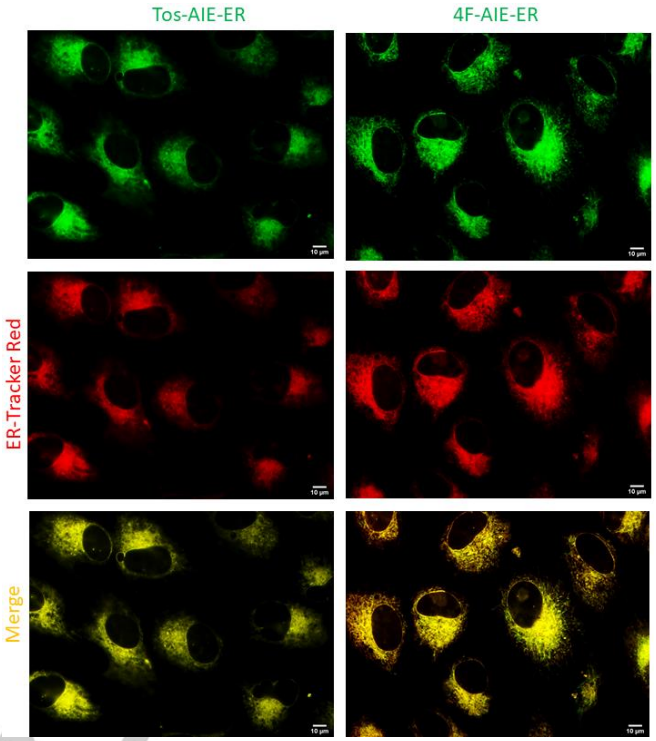

Figure 6. Fluorescence microscopy images of RPE-1 cells incubated with Tos-AIE-ER and 4F-AIE-ER at 20 μM concentration for 1h at 37°C, followed by staining the ER with ER Tracker Red dye. Scale bar = 10 μm.

geometries of both compounds showed the presence of intramolecular dual H-bonding as well as the H-bonded moieties were in the same plane which would trigger the aggregation process to show the AIE property (Figure 4c, d and Figure S29). For successful imaging of sub-cellular ER, the AIE probes should be non-toxic to the cancer cells. Hence, we evaluated the toxicity of Tos-AIE-ER and 4F-AIE-ER in HeLa cervical cancer cells in a dose dependent manner for 24h and calculated the cell viability by MTT assay. Tos-AIE-ER showed negligible cytotoxicity till 20 μM concentration with 96.8 % cell viability (Figure S30a). On the other hand, 4F-AIE-ER demonstrated only 80.3% cell viability at 20 μM (Figure S30b). As result, we have chosen 20 μM concentration for both the compounds for bioimaging of ER in HeLa cells. To fluorescently mark the ER in cancer cells, we treated the HeLa cells with Tos-AIE-ER and 4F-AIE-ER in 20 μM concentration for 1h. We counter stained the ER in HeLa cells with ER-Tracker Red dye and the live cells were visualized by the fluorescence microscopy. The fluorescence microscopy images in Figure 5 evidently showed that Tos-AIE-ER and 4F-AIE-ER (green fluorescence) localized successfully into the ER (red fluorescence) of HeLa cells producing the merged yellow signals within 1h. The high Pearson's coefficient (R= 0.99) of Tos-AIE-ER and 4F-AIE-ER at 1h quantified from the fluorescence microscopy also indicated high colocalization of the AIE probes into the sub-cellular ER. To evaluate the effect of these ER targeting AIE molecules in cancer cells for longer time, we incubated HeLa cells with Tos-AIE-ER and 4F-AIE-ER in a dose dependent manner for 48h and 72h. Interestingly, Tos-AIE-ER showed remarkable killing of HeLa cells with IC_{50} = 4.6 and 2.8 μM at 48h and 72h respectively (Figure S31a, b). Similarly, 4F-AIE-ER also demonstrated HeLa cell killing with IC_{50} = 8.9 and 6.2 μM at 48h and 72h respectively (Figure S31c, d). We anticipate that, these cytotoxicity assays of both the ER targeting AIE probes in HeLa cells at prolonged incubation would open new possibility of theranostic applications which need to be explored further.

We further evaluated the effectiveness of our ER imaging probe in non-cancerous RPE-1 human retinal epithelial cells. We treated RPE-1 cells with Tos-AIE-ER and 4F-AIE-ER at 20 μM concentration for 1h followed by staining the ER with the ER-Tracker Red. We observed the live cells under fluorescence microscopy, which demonstrated that Tos-AIE-ER and 4F-AIE-ER (green fluorescence) localized into the ER of the RPE-1 cells leading to the generation of the merged yellow fluorescence signals within 1h (Figure 6). The effective colocalization of Tos-AIE-ER and 4F-AIE-ER in the ER was quantified with high Pearson's coefficients, R = 0.99 and 0.97 respectively. These fluorescence microscopy images clearly demonstrated that Tos-AIE-ER and 4F-AIE-ER effectively homed into the ER of the cancer and non-cancerous cells within 1h. However, based on the emission wavelength (λ_{max} = 500-512 nm) of both the compounds the imaging capability will only be limited to cellular level. Currently, we are exploring the possibility of extending the emission wavelength of these ER targeting AIE probes towards NIR region for effective tissue and organ imaging.

Conclusion

In conclusion, in this work, we have designed and synthesized γ-resorcylic acid-based probes having sub-cellular ER targeting tags in an easy and succinct manner. These ER targeting small molecules demonstrated remarkable aggregation induced emission property in water as well as in solid state by dual-intramolecular H-bonding. These AIE active ER targeting probes

efficiently homed into and illuminated ER in HeLa cancer cells as well as RPE-1 human retinal epithelial cells within 1h. To the best of our knowledge, this is the first example of dual intramolecular H-bonded small molecule AIEgens for illuminating ER in the sub-cellular milieu. We envisage that, these novel small molecule AIEgens have potential to unravel chemical biology of ER as well as in future theranostic applications.

Acknowledgements

S.B. sincerely thanks IIT Gandhinagar for internal funding, Gujarat Council on Science and Technology (GUJCOST/STI/R&D/2020-21/1302) and Science and Engineering Research Board (CRG/2020/001127) for financial support. J.I. and C.M. acknowledge IIT Gandhinagar for doctoral fellowship. D.B thanks SERB, GoI for Ramanujan fellowship and IITGN, DBT-EMR, GUJCOST and GSBTM for research grants. A.M. acknowledges IITGN for computational support.

Conflict of interest

The authors declare no conflict of interest.

Keywords: hydrazide-hydrazone• aggregation induced emission• intramolecular dual H-bonding • endoplasmic reticulum.

[1] M. Wang, R. J. Kaufman, *Nat. Rev.,* **2016**, *529*, 326-335.

[2] P. Pizzo, T. Pozzan, *Trends Cell Biol.,* **2007**, *17*, 511-517.

[3] T. Anelli, R. Sitia, *Embo j.,* **2008**, *27*, 315-327.

[4] T. Avril, E. Vauléon, E. Chevet, *Oncogenesis,* **2017**, *6*, e373.

[5] M. H. Smith, H. L. Ploegh, J. S. Weissman, *Science,* 2011, *334*, 1086-1090.

[6] R. Bravo, V. Parra, D. Gatica, A. E. Rodriguez, N. Torrealba, F. Paredes, Z. V. Wang, A. Zorzano, J. A. Hill, E. Jaimovich, A. F. Quest, S. Lavandero, *Int. Rev. Cell Mol. Biol.,* **2013**, *301*, 215-290.

[7] C. Y. Liu, R. J. Kaufman, *J. Cell Sci*., **2003**, *116*, 1861-1862.

[8] C. Hetz, F. R. Papa, *Mol. Cell,* **2018**, *69*, 169-181.

[9] H. Urra, E. Dufey, T. Avril, E. Chevet, C. Hetz, *Trends Cancer,* **2016**, *2*, 252-262.

[10] H. J. Clarke, J. E. Chambers, E. Liniker, S. J. Marciniak, *Cancer Cell,* **2014**, *25*, 563-573.

[11] S. S. Cao, R. J. Kaufman, *Antioxid, Redox Signal.,* **2014**, *21*, 396-413.

[12] J. Lee, U. Ozcan, *J. Biol. Chem.,* **2014**, *289*, 1203-1211.

[13] H. Zhang, J. Hu, *Trends Cell Biol.,* **2016**, *26*, 934-943.

[14] L. M. Westrate, J. E. Lee, W. A. Prinz, G. K. Voeltz, *Annu. Rev. Biochem.,* **2015**, *84*, 791-811.

[15] a) H. Zhang, J. Fan, H. Dong, S. Zhang, W. Xu, J. Wang, P. Gao, X. Peng, *J. Mater. Chem. B.,* **2013**, *1*, 5450-5455.

[16] S. Phaniraj, Z. Gao, D. Rane, B. R. Peterson, *Dyes Pigm.,* **2016**, *135*, 127-133.

[17] J. M. Meinig, L. Fu, B. R. Peterson, *Angew. Chem. Int. Ed.,* **2015**, *54*, 9696-9699.

[18] M. S. T. Gonçalves, *Chem. Rev.,* **2009**, *109*, 190-212.

[19] Q. Yang, Z. Ma, H. Wang, B. Zhou, S. Zhu, Y. Zhong, J. Wang, H. Wan, A. Antaris, R. Ma, X. Zhang, J. Yang, X. Zhang, H. Sun, W. Liu, Y. Liang, H. Dai, *Adv. Mater.,* **2017**, *29,* 1605497.

[20] R. Zuzak, R. Dorel, M. Krawiec, B. Such, M. Kolmer, M. Szymonski, A. M. Echavarren, S. Godlewski, *ACS Nano,* **2017**, *11*, 9321-9329.

[21] a) C. Zhu, R. T. K. Kwok, J. W. Y. Lam, B. Z. Tang, *ACS Appl. Bio Mater.,* **2018**, *1*, 1768-1786.

[22] J. Liang, B. Z. Tang, B. Liu, *Chem. Soc. Rev.,* **2015**, *44*, 2798-2811.

[23] D. Ding, K. Li, B. Liu, B. Z. Tang, *Acc. Chem. Res.,* **2013**, *46*, 2441-2453.

[24] J. Qian, B. Z. Tang, *Chem.,* **2017**, *3*, 56-91.

[25] Y. Hong, J. W. Y. Lam, B. Z. Tang, *Chem. Commun.,* **2009**, 4332-4353.

[26] Y. Hong, J. W. Y. Lam, B. Z. Tang, *Chem. Soc. Rev.,* **2011**, *40*, 5361-5388.

[27] D. Ding, K. Li, B. Liu, B. Z. Tang, *Acc. Chem. Res.,* **2013**, *46*, 2441-2453.

[28] D. Wang, H. Su, R. T. K. Kwok, X. Hu, H. Zou, Q. Luo, Michelle M. S. Lee, W. Xu, J. W. Y. Lam, B. Z. Tang, *, Chem. Sci.,* **2018**, *9*, 3685-3693.

[29] C. W. T. Leung, Y. Hong, S. Chen, E. Zhao, J. W. Y. Lam, B. Z. Tang, *J. Am. Chem. Soc.,* **2013**, *135*, 62-65.

[30] F. Hu, X. Cai, P. N. Manghnani, Kenry, W. Wu, B. Liu, *Chem. Sci.,* **2018**, *9*, 2756-2761.

[31] D. Wang, H. Su, R. T. K. Kwok, G. Shan, A. C. S. Leung, M. M. S. Lee, H. H. Y. Sung, I. D. Williams, J. W. Y. Lam, B. Z. Tang, *Adv. Funct. Mater.,* **2017**, *27*, 1704039.

[32] Y. Cheng, C. Sun, X. Ou, B. Liu, X. Lou, F. Xia, *Chem. Sci.,* **2017**, *8*, 4571-4578.

[33] P. Alam, W. He, N. L. C. Leung, C. Ma, R. T. K. Kwok, J. W. Y. Lam, H. H. Y. Sung, I. D. Williams, K. S. Wong, B. Z. Tang, *Adv. Funct. Mater.,* **2020**, *30*, 1909268.

[34] Z. Zhu, Q. Wang, H. Liao, M. Liu, Z. Liu, Y. Zhang, W.-H. Zhu, *Natl. Sci. Rev.,* **2020**, *8*. nwaa198.

[35] P. Xiao, K. Ma, M. Kang, L. Huang, Q. Wu, N. Song, J. Ge, D. Li, J. Dong, L. Wang, D. Wang, B. Z. Tang, *Chem. Sci.,* **2021**, *12*, 13949-13957.

[36] S. Patil, S. Pandey, A. Singh, M. Radhakrishna, S. Basu, *Chem. Eur. J.,* **2019**, *25*, 8229-8235.

[37] C. Ghosh, A. Nandi, S. Basu, *ACS Appl. Bio Mater.*, **2019**, *2*, 3992−400.

[38] Y. Tang, A. Xu, Y. Ma, G. Xu, S. Gao, W. Lin, Sci. Rep. 2017, 7, 12944.

[39] J. Hou, H. S. Kim, C. Duan, M. S. Ji, S. Wang, L. Zeng, W. X. Ren, J. S. Kim, *Chem. Commun.*, **2019**,*55*, 2533-2536.

[40] A. Goujon, A. Colom, K. Straková, V. Mercier, D. Mahecic, S. Manley, N. Sakai, A. Roux, S. Matile, *J. Am. Chem. Soc.* **2019**, *141*, 3380−3384.

[41] S. Ghosh, S. Nandi, C. Ghosh, K. Bhattacharyya, *ChemPhysChem.*, **2016**,*17*, 2818-2823.

[42] Q. Yuan, T. Zhou, L. Li, J. Zhang, X. Liu, X. Ke, A. Zhang, *RSC Adv.,* **2015**, *5*, 31153-31165.

[43] Gaussian 09, Revision D. 01, M. J. Frisch, G. W. Trucks, H. B. Schlegel, G. E. Scuseria, M. A. Robb, J. R. Cheeseman, G. Scalmani, V. Barone, B. Mennucci, G. A. Petersson, H. Nakatsuji, M. Caricato, X. Li, H. P. Hratchian, A. F. Izmaylov, J. Bloino, G. Zheng, J. L. Sonnenberg, M. Hada, M. Ehara, K. Toyota, R. Fukuda, J. Hasegawa, M. Ishida, T. Nakajima, Y. Honda, O. Kitao, H. Nakai, T. Vreven, J. A. Montgomery, Jr., J. E. Peralta, F. Ogliaro, M. Bearpark, J. J. Heyd, E. Brothers, K. N. Kudin, V. N. Staroverov, R. Kobayashi, J. Normand, K. Raghavachari, A. Rendell, J. C. Burant, S. S. Iyengar, J. Tomasi, M. Cossi, N. Rega, J. M. Millam, M. Klene, J. E. Knox, J. B. Cross, V. Bakken, C. Adamo, J. Jaramillo, R. Gomperts, R. E. Strat- mann, O. Yazyev, A. J. Austin, R. Cammi, C. Pomelli, J. W. Ochterski, R. L. Martin, K. Morokuma, V. G. Zakrzewski, G. A. Voth, P. Salvador, J. J. Dannenberg, S. Dapprich, A. D. Daniels, Ö. Farkas, J. B. Foresman, J. V. Ortiz, J. Cioslowski, D. J. Fox, Gaussian. Inc., Wallingford, CT, USA **2013**.

[44] P. J. Stephens, F. J. Devlin, C. F. N. Chabalowski, M. J. Frisch, *J. Phys. Chem.* **1994**, *98*, 11623-11627.

[45] A. V. Marenich, C. J. Cramer, D. G. Truhlar, *J. Phys. Chem. B*, **2009**, *113*, 6378-6396.

10.1002/chem.202200203

WILEY-VCH

RESEARCH ARTICLE

Entry for the Table of Contents

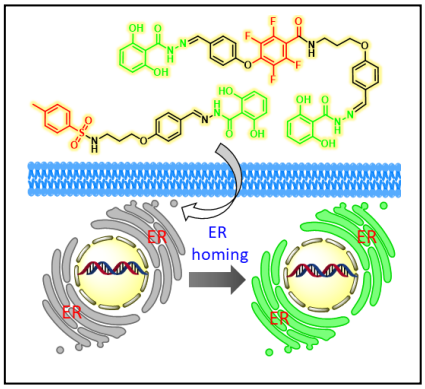

Illuminate ER. Two small molecules with γ-resorcyclic acid moiety were designed and synthesized having aggregation-induced emission (AIE) activity due to dual intramolecular H-bonding. These small molecules localized into the sub-cellular endoplasmic reticulum to light it up.